Scientific Research Publishing

Open Journal of Applied Sciences, 2025, 15(6), 1853-1870
https://www.scirp.org/journal/ojapps
ISSN Online: 2165-3925
ISSN Print: 2165-3917

Support Vector Regression Methodology for Performance Prediction of an Automotive Torque Converter with Turbine Parametric Model

Jie Chen*, Yifan Qiu

How to cite this paper: Chen, J. and Qiu, Y.F. (2025) Support Vector Regression Methodology for Performance Prediction of an Automotive Torque Converter with Turbine Parametric Model. *Open Journal of Applied Sciences*, **15**, 1853-1870.
https://doi.org/10.4236/ojapps.2025.156124

Received: May 7, 2025
Accepted: June 27, 2025
Published: June 30, 2025

Abstract

Support vector regression (SVR) and computational fluid dynamics (CFD) techniques are applied to predict the performance of an automotive torque converter in the design process of turbine geometry. A new parametric geometric model of turbine is proposed by means of parametric equations and Creo software to improve the design efficiency. The validity of the parametric design method and the accurateness of numerical analysis are verified by comparing simulation results with experimental data. Orthogonal design and latin hypercube design (LHD) methods are used to obtain the train data and test data, respectively, for SVR. To build an effective SVR model, the SVR parameters are optimized employing cross-validation and grid search methods. Polynomial and radial basis function (RBF) are applied as the kernel function of SVR for predicting converter performance characteristics, including stall torque ratio and peak efficiency. Instead of minimizing the observed training error, SVR with polynomial kernel and SVR with RBF kernel attempt to minimize the generalization error bound so as to achieve generalized performance. The results show that SVR methodology can serve as an effective approach to predict the performance of torque converters.

Keywords

Support Vector Regression, Performance Prediction, Automotive Torque Converter, Computational Fluid Dynamics, Parametric Geometric Model

1. Introduction

The torque converter is an important component in an automatic transmission.

It provides automatic torque amplification according to the different rotational speed between the input and output speeds without any active control, inherently suppressing engine torque fluctuations [1]. An impeller, a turbine, and a stator all are a part of a torque converter. The impeller energizes the working oil and is connected to the engine, while the turbine extracts energy from the fluid and drives the transmission shaft. Flow field in turbine passage is quite complex for the reason that the rotation speed of turbine changes with the speed ratio changes. To get a larger torque ratio at low speed ratio, the turbine blade angles always change drastically. Therefore, it is very important to understand the relationship between turbine geometrical parameters and the performance characteristics of a torque converter. This knowledge will greatly help designers to improve the torque converter performance.

It is generally been accepted that while the accuracy of computational fluid dynamics (CFD) analyses has not yet achieved a level that is equivalent to experimental techniques, its ability to correctly predict the direction of any changes is reliable [2]. In recent years, CFD has been widely used in turbomachinery design and optimization. Rutter *et al.* [3] investigated the hydraulic performance of a centrifugal pump within the electrical submersible pump (ESP) unit in single-phase flow using CFD technique. Zhao *et al.* [4] optimized a double-channel pump's impeller by combined using of CFD, multi-objective genetic algorithm (MOGA) and artificial neural networks (ANN). Shojaeefard *et al.* [5], and Bellary *et al.* [6], improved the performance of a centrifugal pump impeller based on CFD simulations. Hur *et al.* [7] analyzed the flow and performance of a partially-charged water retarder by CFD. Many researchers have also studied the flows in torque converters by using CFD codes employing various methods [8]-[10].

Recently, support vector machine (SVM) has been extensively applied to various areas to overcome the problem of non-linear relationships and predictions [11]-[13]. There are two main categories for support vector machines: support vector classification (SVC) and support vector regression (SVR). SVM is a learning system using high-dimensional features. SVR is based on statistical learning theory and a structural risk minimization principle, which has been successfully used for non-linear system modeling. Rajasekaran *et al.* [14] applied support vector regression methodology for storm surge predictions. Bermolen, *et al.* explored the use of SVR for the purpose of link load forecast. Shamshirband, *et al.* [15] presented the SVR methodology for sensor data fusion to improve tracking abililty. Taghavifar *et al.* [16] optimized the injection strategy-chamber geometry of diesel engine using DOE method incorporating with the SVR to predict output parameters with acceptable accuracy. Although several studies [17]-[20] were reported using various methods to predict torque converter performance, application of SVR method to predict torque converter performance is scarce.

A kernel function can be utilized to form qualified function that is used SVM. Researchers have demonstrated the use of SVR in predicting hydrological model-

ing and pointed out the positive performance of the RBF (radial basis function) [21] [22]. Asefa *et al.* [23] proposed different kernels in SVR to rainfall-runoff modeling and validated that the radial basis function (RBF) outperforms other kernel functions. In this paper, the SVR for prediction of the torque converter performance including stall torque ratio and peak efficiency is applied, with two kernel functions being investigated, namely RBF and polynomial kernel function.

The basic idea behind the SVR methodology is to collect input/output data pairs and to learn the proposed network from these data. In our scheme, the input data comes from design parameters of turbine geometry for an automotive torque converter. Design of experiment (DOE) together with CFD techniques is used to obtain the output data. To improve the design efficiency, a new parametric geometric design method of turbine is proposed by using parametric equations and Creo software.

2. Parametric Model of Turbine

2.1. Torus Design

The turbine parametric design starts with the definition of the torus shape. Various design parameters, including active diameter, aspect ratio and two arc radii are needed to determine the shell profile of an automotive torque converter torus. As the flow area in the circular path, in the proposed torque converter model, is assumed constant, only the design parameter area factor f_a is used to determine the design path and core of torus. Consequently, by defining the turbine inlet radius R_1 and outlet radius R_2, along with the shell and core, the torus profile of turbine can be obtained as shown in **Figure 1**.

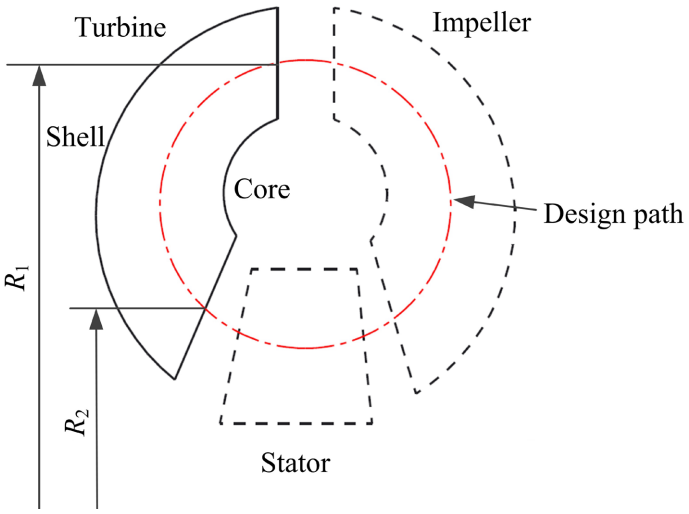

Figure 1. Torus profile of turbine.

2.2. Blade Design

Each turbine blade profile is formed by a three dimensional (3D) curve of the shell and a 3D curve of the core. The 3D curve can be calculated from the torus and a

two dimensional (2D) design curve using the conformal transformation principle. Figure 2 shows the schematic representation of a 2D design curve. With the origin at the starting point of the curve, the coordinate of P_0 is (0, 0). The curve expression can be written with the following equation:

$$Ax^2 + By^2 + Cx + Dy + Exy = 0 \tag{1}$$

where A, B, C, D and E are the coefficients of the variables. It should be noted that the value of D is 1.0 and the parametric equation of the 2D design curve can be obtained as

$$Ax_1^2 + By_1^2 + Cx_1 + y_1 + Ex_1y_1 = 0 \tag{2}$$

$$Ax_2^2 + By_2^2 + Cx_2 + y_2 + Ex_2y_2 = 0 \tag{3}$$

$$\tan(\alpha_1 - 90) + C = 0 \tag{4}$$

$$(Ex_2 + 2By_2 + 1)\tan(\alpha_2 - 90) + 2Ax_2 + Ey_2 + C = 0 \tag{5}$$

where α_1 is the inlet angle of turbine, and α_2 is the exit angle of turbine. In the present study, four design parameters including inlet angle α_1, exit angle α_2, offset size d, and conic factor f_c are provided to calculate the 2D design curve. The coordinates of P_c and P_1 can be obtained as

$$y_c = x_c \tan(\alpha_1 - 90) \tag{6}$$

$$y_c = y_2 - (x_2 - x_c)\tan(\alpha_2 - 90) \tag{7}$$

$$x_1 = x_2/2 + (x_c - x_2/2) f_c \tag{8}$$

$$y_1 = y_2/2 + (y_c - y_2/2) f_c \tag{9}$$

where $P_c(x_c, y_c)$ is the intersection of the two tangent lines that across the curve's starting and ending points, respectively (Figure 2). According to the definition of 2D design curve, x_2 value and y_2 value equal to the length of torus l and offset size d, respectively.

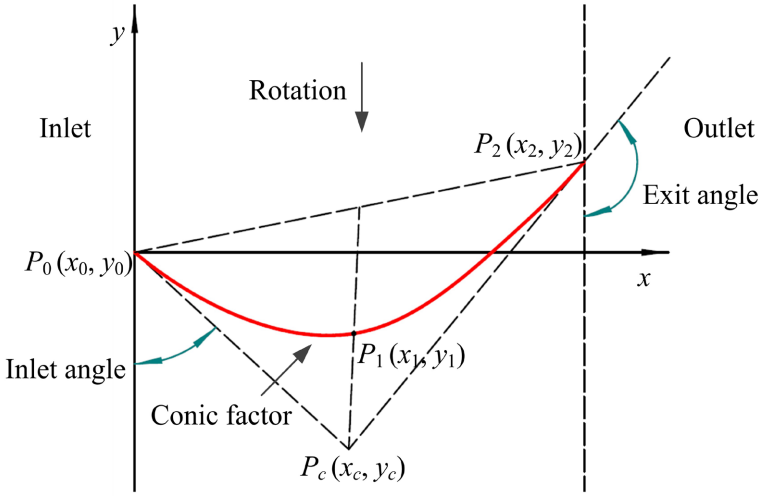

Figure 2. Schematic representation of 2D design curve.

The 2D design curve can be easily constructed by having the torus and the four design parameters defined. After the definition of 3D curves of shell and core, another design parameter bias angle β is used to obtain the blade profile. Given the turbine blades are constant-thickness stamped sheet metal, the blade thickness t is defined. Once the torus shape and five blade design parameters including inlet angle α_1, exit angle α_2, offset size d, conic factor f_c, bias angle β and blade thickness t are determined, the basic blade geometry of turbine is generated by means of parametric equations and Creo software. The schematic representation of the construction of turbine blade is shown in Figure 3.

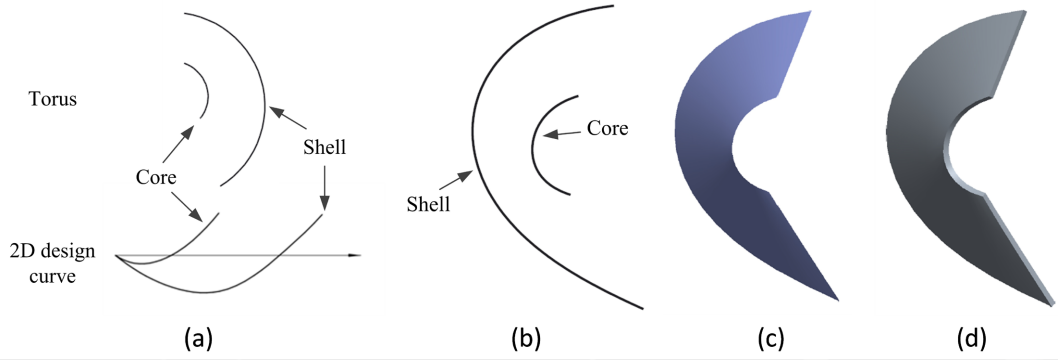

Figure 3. Schematic representation of the construction of turbine blade: (a) 2D design curve for turbine blade, (b) 3D curve of turbine, (c) blade profile of turbine, (d) blade geometry of turbine.

After the definition of the torus and a blade, the construction of the whole turbine geometry is easy and is based on the rotation of the generic blade around the axis; for doing so the number of blades z should be provided by the user. The completed turbine parametric geometry is shown in Figure 4. The design parameters considered for the parametric study are shown in Table 1, provided that the torus of turbine is determined.

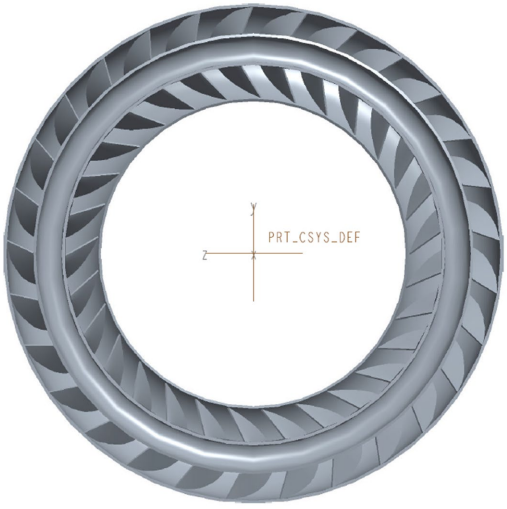

Figure 4. Turbine parametric geometry.

Table 1. Parameters of turbine.

No.	Description	Parameter
1	Exit angle of turbine at shell (˚)	α_{s1}
2	Inlet angle of turbine at shell (˚)	α_{s2}
3	Conic factor of turbine blade at shell	f_{cs}
4	Offset size of turbine blade at shell (mm)	d_s
5	Exit angle of turbine at core (˚)	α_{c1}
6	Inlet angle of turbine at core (˚)	α_{c2}
7	Conic factor of turbine blade at core	f_{cc}
8	Offset size of turbine blade at core (mm)	d_c
9	Bias angle of turbine (˚)	β
10	Blade number of turbine	z
11	Blade thickness of turbine (mm)	t

3. Model Verification

3.1. Computational Approach

An automotive torque converter is selected as a reference to generate the parametric model. The reference torque converter has an active diameter of 250 mm and the number of blades in the impeller, turbine, and stator are 31, 29, and 21, respectively. STAR-CCM+ software is used to generate the computational mesh and perform the internal flow calculations appropriately. The computational mesh is given in Figure 5, where only one blade passage is modeled for each element to illustrate the mesh distribution in the computational field when approximately 103, 533 grid cells in total are used. The polyhedral cells with five prism layers is used on the model. The leakage between the elements and also between an element and the core flow is disregarded. A cyclic boundary condition is imposed on both peripheral boundaries outside a blade passage. A no-slip wall boundary condition is also imposed on all the walls bounding the domain,

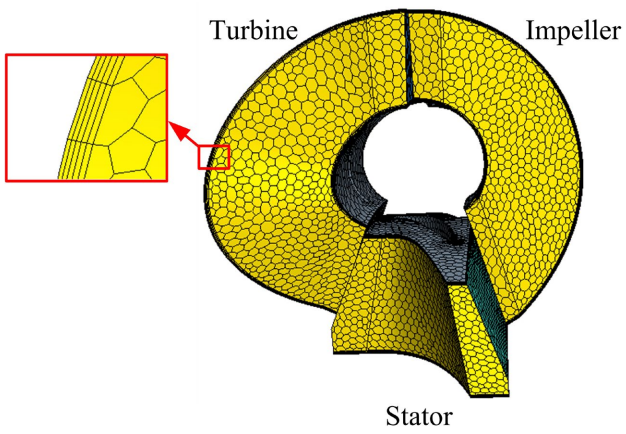

Figure 5. Torque converter grid model.

with a spin applied as necessary. The interfaces between elements have been handled by using the mixing plane method. A second-order upwind differencing scheme is utilized and the SST *k-w* model is also used for the turbulence. Steady state simulations are performed for a range of speed ratios from 0.0 to 0.9 while maintaining an impeller speed of 2000 rpm.

3.2. Comparison between Simulation and Experimental Results

Figure 6 compares the measured and calculated overall performance including efficiency η, torque ratio Tr, and impeller torque factor λ_I for the parametric model of the torque converter. As indicated here, the tendencies of the experimental data correlated relatively well with the calculated results, confirming that the parametric model and computational method are valid in general. It is of note that the CFD underestimates the impeller torque factor λ_I at low speed ratios. The discrepancy between measurements and calculations are reasonable because of the overestimated incidence losses at low speed ratios.

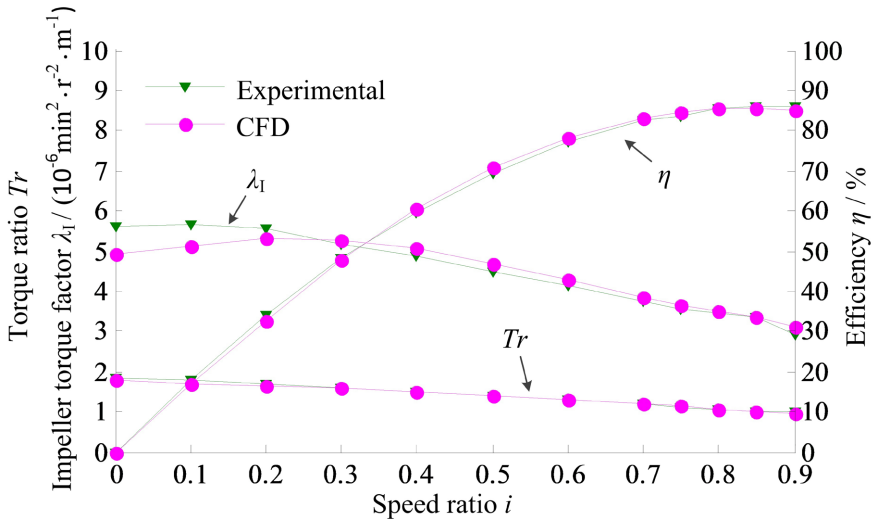

Figure 6. Comparison of the CFD calculation analysis with experimental results.

4. Data Collection and Support Vector Regression (SVR)

4.1. Input Parameters

The ability of the SVR to make reasonable estimations is mostly dependent on input parameters selection. Adequate consideration of the factors of turbine effecting the torque converter performance studied is therefore crucial to developing a reliable network. As mentioned above, 11 design parameters are used to obtain an turbine parametric model. Blade scroll angle γ is introduced as another design parameter to investigate the effect of the turbine geometry on the performance of a torque converter. The scroll angle is defined as the angle between the two planes containing the intersection of the design path and the entering and leaving edges of the blade when that blade does not lie in one axial plane. The scroll angle can be determined by four design parameters including inlet angle α_1, exit angle α_2,

conic factor f_c, and offset size d, provided that the torus is defined. Matlab software is used to develop a simple-to-use GUI to calculate scroll angle as shown in Figure 7.

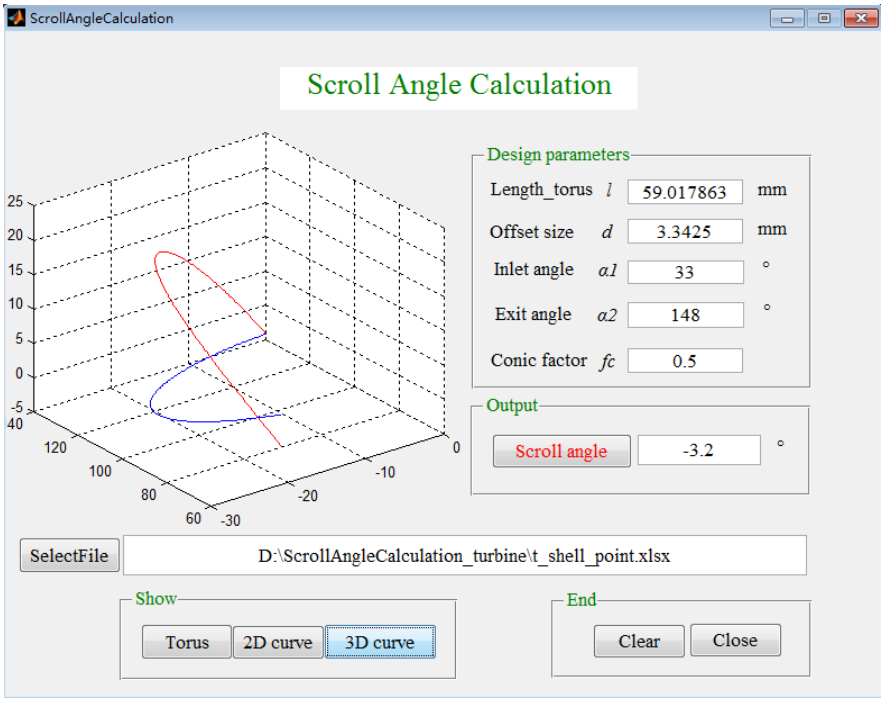

Figure 7. GUI interface used for scroll angle calculation.

The blade scroll angles at shell and core can be represented by the mean scroll angle and change simultaneously with the change of the mean value. Similarly, the inlet angles and exit angles at shell and core can also be represented by the mean value of inlet angle and mean exit angle. Finally, the 11 design parameters of turbine are translated into 6 parameters including inlet angle α_1, exit angle α_2, scroll angle γ, bias angle β, blade thickness t, and blade number z. The six design parameters are to be defined as input for the learning techniques in this research study. The range of design parameters and base values of the turbine are summarized in Table 2.

Table 2. Range of design parameters and base values of the turbine.

Design parameters	Base value	Range of variation
Blade number z	29	25 - 33
Blade thickness t /mm	1	0.9 - 1.3
Bias angle β /(˚)	2.75	−1 - 5
Scroll angle γ /(˚)	−1.035	−3 - 1
Inlet angle α_1 /(˚)	34.75	25 - 45
Exit angle α_2 /(˚)	150.75	140 - 160

4.2. Design of Experiment (DOE)

4.2.1. Orthogonal Design Approach

Orthogonal design approach is a collection of mathematical and statistical techniques to reduce the number of experiments in order to find the effect of parameters affecting a response in a process, thereby aiming for a reduction in both costs and time. Orthogonal design sets out configurations (or arrangements) to be conducted using an appropriate orthogonal array; the terminology used in these arrays includes "factors" —an item that is to be varied during the simulations, "level" —the number of times a factor is to be varied during the simulations and "configuration number" —the number of simulations that are required to be run to complete the analysis [24]. For this paper six main geometrical parameters mentioned above are selected as design variables (factors) and five different values (levels) are assigned for each design parameter. So 25 ($L_{25}[5^6]$) configurations with different combinations are generated for orthogonal design. Stall torque ratio Tr_0 and peak efficiency η^* are used as the dynamic characteristic and economic characteristic, respectively, to evaluate the performance of torque converters. The above mentioned CFD simulation method is applied and the corresponding calculation results for 25 cases are presented in Figure 8. The 25 sets of calculation data are used for SVR modeling training.

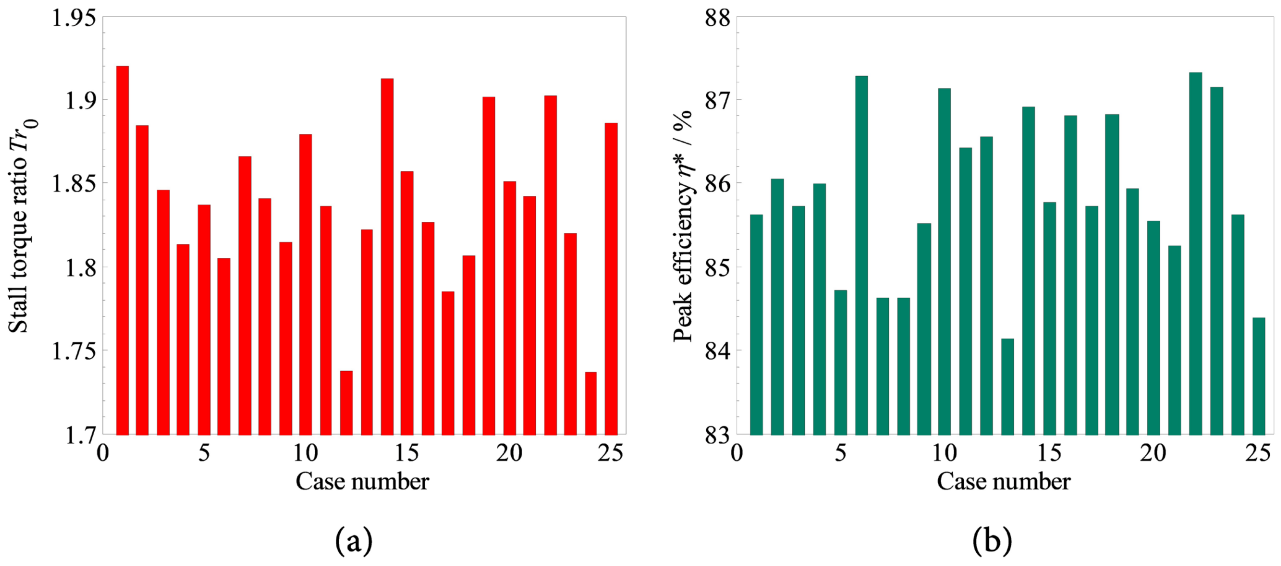

Figure 8. (a) Stall torque ratio and (b) peak efficiency for all designed cases.

4.2.2. Latin Hypercube Design (LHD)

The Latin Hypercube design is a popular choice of experimental design when computer simulation is used to study a physical process. These designs guarantee uniform samples for the marginal distribution of each single input [25]. Five cases are obtained using LHD method and the corresponding calculation results are shown in Figure 9. The 5 sets of data as testing data to analyze the prediction performance of SVR.

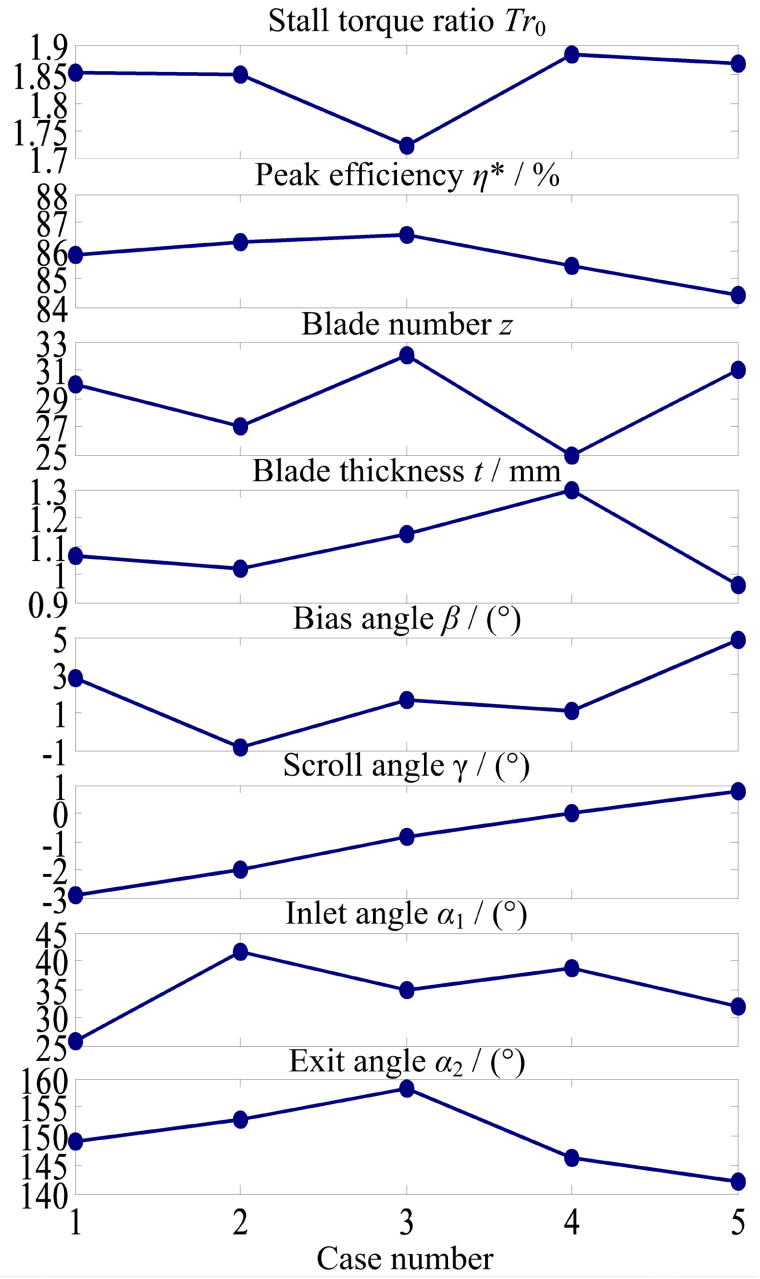

Figure 9. Design variables and indicators.

4.3. Support Vector Regression (SVR)

SVR in its essence is closely related with SVM theory and its parameters such as kernel and operating process are not disparate. The ε-insensitive loss function is the most widely used cost function. It can be assumed as a tube equal to the approximation accuracy that surrounds the training data [26]. The objective held by SVR is to search for the function with the most ε deviations from the real destination vector for all training information received and which must be as flat as possible [27]. For linear regression problems, the regression model can be expressed by Vapnik [28] and is defined by the following function:

$$f(x)=\langle w,x\rangle+b \tag{10}$$

where $f(x)$ is an unknown target function, $\langle .,. \rangle$ denotes the dot product and w is the weight vector. The ε -insensitive loss function is defined by the following function:

$$L_{\varepsilon}(y)=\begin{cases}0, & \text{for } |f(x)-y|\le\varepsilon\\ |f(x)-y|-\varepsilon, & \text{otherwise}\end{cases} \tag{11}$$

As a convex optimization problem, it can be written as:

$$\text{Minimize } \frac{1}{2}\|w\|^2+C\sum_{i=1}^{l}\left(\xi_i+\xi_i^*\right) \tag{12}$$

$$\text{Subject to } \begin{cases}y_i-\langle w,x_i\rangle-b\le\varepsilon+\xi_i\\ \langle w,x_i\rangle+b-y_i\le\varepsilon+\xi_i^*\\ \xi_i,\xi_i^*\ge 0\end{cases} \tag{13}$$

where ξ_i and ξ_i^* variables are to satisfy the function constraints. The corresponding dual optimization problem is defined as [29]:

$$\max_{\alpha,\alpha^*}-\frac{1}{2}\sum_{i=1}^{l}\sum_{j=1}^{l}\left(\alpha_i^*-\alpha_i\right)\left(\alpha_j^*-\alpha_j\right)\langle x_i,x_j\rangle-\sum_{i=1}^{l}y_i\left(\alpha_i^*-\alpha_i\right)-\varepsilon\sum_{i=1}^{l}\left(\alpha_i^*+\alpha_i\right) \tag{14}$$

with constraints:

$$0\le\alpha_i,\alpha_i^*\le C,i=1,\cdots,l$$

$$\sum_{i=1}^{l}\left(\alpha_i-\alpha_i^*\right)=0 \tag{15}$$

where α_i and α_i^* are Lagrange variables while w and b are denoted by the following equation and x_r and x_s are support vectors [28].

$$w=\sum_{i=1}^{l}\left(\alpha_i^*-\alpha_i\right)x_i$$

$$b=-\frac{1}{2}\langle w,(x_r+x_s)\rangle \tag{16}$$

For nonlinear regression problems, a nonlinear mapping ϕ of the input space onto a higher dimension feature space can be used, and then linear regression can be performed in this space [30], the nonlinear model is written as

$$f(x)=\langle w,\phi(x)\rangle+b \tag{17}$$

where

$$w=\sum_{i=1}^{l}\left(\alpha_i-\alpha_i^*\right)\phi(x_i) \tag{18}$$

$$\langle w,\phi(x)\rangle=\sum_{i=1}^{l}\left(\alpha_i-\alpha_i^*\right)\langle\phi(x_i),\phi(x)\rangle=\sum_{i=1}^{l}\left(\alpha_i-\alpha_i^*\right)K(x_i,x) \tag{19}$$

$$b=-\frac{1}{2}\sum_{i=1}^{l}\left(\alpha_i-\alpha_i^*\right)\left(K(x_i,x_r)+K(x_i,x_s)\right) \tag{20}$$

where x_r and x_s are support vectors.

In this paper, the non-linear RBF kernel and polynomial kernel are investigated and are defined as [31]:

$$\text{RBF:}\quad K\left(x_i, x_j\right) = \exp\left(-\gamma \left\| x_i - x_j \right\|^2\right), \quad \gamma > 0 \tag{21}$$

$$\text{Polynomial:}\quad K\left(x_i, x_j\right) = \left(\gamma x_i^{\mathrm{T}} x_j + r\right)^d, \quad \gamma > 0 \tag{22}$$

where γ, r, and d are kernel parameters.

4.4. Model Performance Evaluation Criteria

The root mean square error RMSE and correlation coefficient R are used to estimate the accuracy of the prediction model:

$$\text{RMSE} = \sqrt{\frac{\sum_{i=1}^{n}\left(y_{\text{sim}} - y_{\text{pre}}\right)^2}{n}} \tag{23}$$

$$R = \frac{\sum_{i=1}^{n}\left(y_{\text{sim}} - \overline{y_{\text{sim}}}\right)\left(y_{\text{pre}} - \overline{y_{\text{pre}}}\right)}{\sqrt{\sum_{i=1}^{n}\left(y_{\text{sim}} - \overline{y_{\text{sim}}}\right)^2 \sum_{i=1}^{n}\left(y_{\text{pre}} - \overline{y_{\text{pre}}}\right)^2}} \tag{24}$$

in which y_{sim} is the value of simulation and y_{pre} is the value of prediction.

5. Results and Discussion

A series of simulation have been conducted for SVR modeling and prediction, and the training data sets and testing data sets used in this paper are obtained using orthogonal design approach and LHD method, respectively. In order to eliminate dimension differences, min/max normalization method is used for data standardization and normalization and then all input and output data are standardized and normalized to the range [0, 1].

5.1. SVR Parameters Optimization

The SVR parameters must be set carefully in order to construct the SVR model efficiently [32]-[34]. Inappropriately chosen SVR parameters will result in over-fitting or under-fitting, and different parameter settings may also cause significant differences in performance [35]. Thus, selecting the optimal parameters is an important step in SVR design. Cross-validation together with grid-search method is applied to obtain the SVR optimal parameters. In v-fold cross-validation, we first divide the training set into v subsets of equal size. Sequentially one subset is tested using the classifier trained on the remaining $v-1$ subsets. Thus, each instance of the whole training set is predicted once so the cross-validation accuracy is the percentage of data that are correctly classified [31]. In our scheme, 5-fold cross validation is selected and the values of epsilon and tolerance are 0.01 and 0.001 seem to perform well. To select optimal combinations of C and γ for radial basis function kernels, a coarse grid-search is used first. The contours of

coarse grid search results for stall torque ratio and peak efficiency predictions are shown in Figure 10.

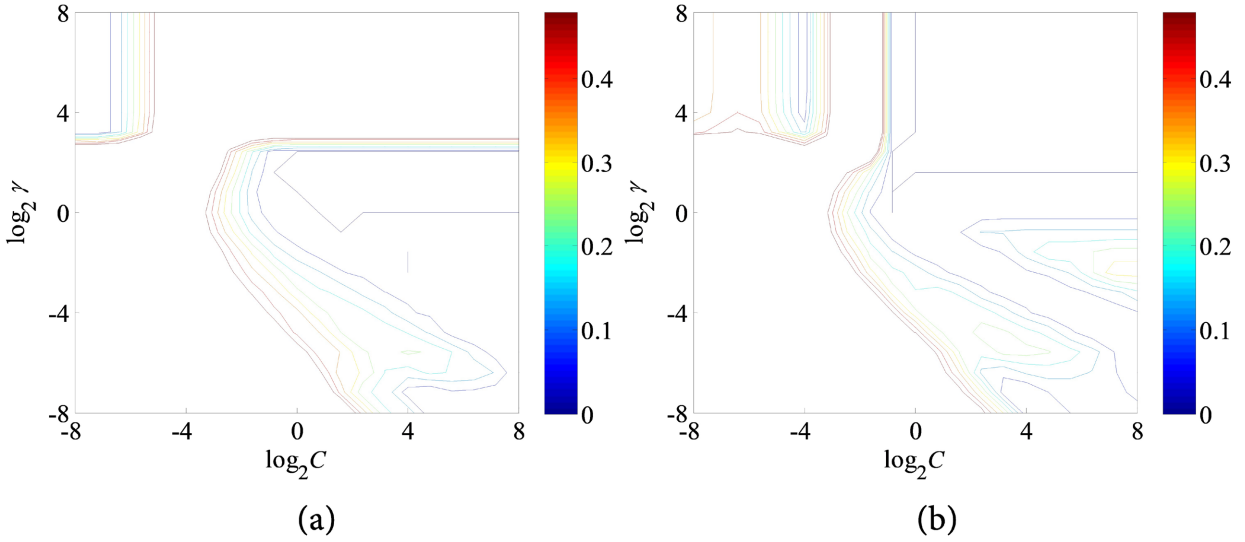

Figure 10. Coarse grid search results for (a) stall torque ratio and (b) peak efficiency predictions.

After identifying a "better" region on the grid, a finer grid search on that region can be conducted. The three dimensional plot of finer grid search results for stall torque ratio and peak efficiency predictions are presented in Figure 11.

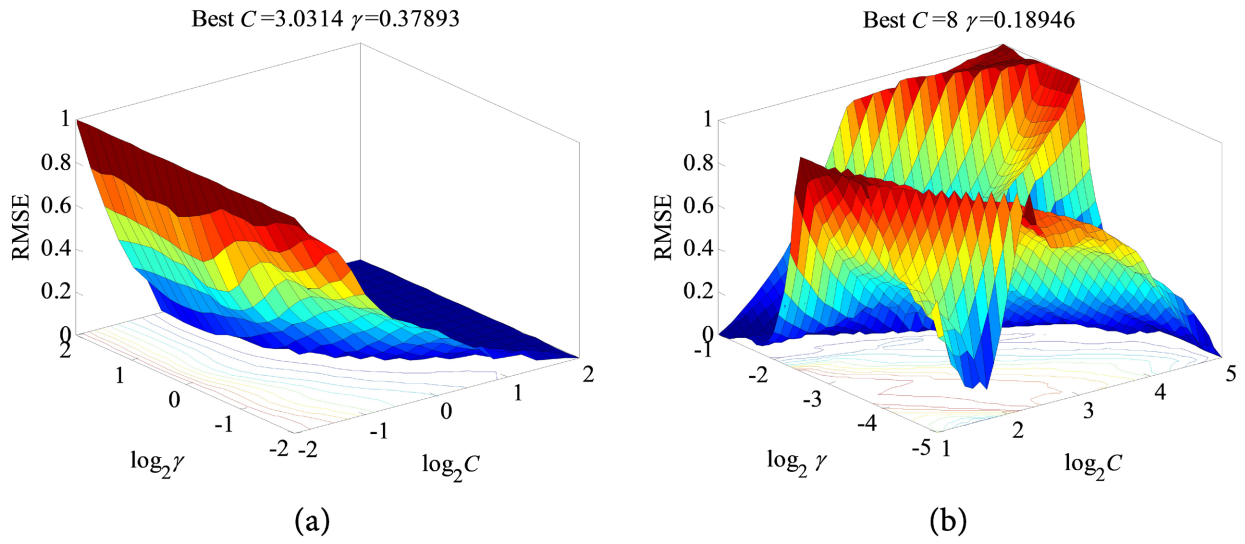

Figure 11. Finer grid search results for (a) stall torque ratio and (b) peak efficiency predictions.

It can be seen that the grid optimization process for stall torque ratio yields to a minimum RMSE when $(C,\gamma)=(3.0314,0.37893)$ while the best (C,γ) for peak efficiency is (4.5948, 0.26794). The similar grid-search method is also employed for SVR with polynomial kernel function. Table 3 provides the optimal values of parameters for this data set with polynomial and RBF kernel-based SVR.

Table 3. Optimal parameters for SVR with RBF and polynomial function.

SVR parameters	Stall torque ratio Tr_0		Peak efficiency η^* /%	
	RBF	Polynomial	RBF	Polynomial
Epsilon value ε	0.1	0.1	0.1	0.1
Cost value C	3.0314	0.125	8	0.022097
Tolerance value ξ	0.001	0.001	0.001	0.001
Degree of kernel d	-	2	-	2
Gamma value of kernel γ	0.37893	0.75786	0.18946	7.4643
Coefficient value of kernel r	-	0	-	0

5.2. SVR Prediction

The training data is used to establish the RBF and polynomial kernel-based SVR model for stall torque ratio and peak efficiency predictions. Results in Figure 12 and Figure 13 compare the RBF based SVR (SVR_rbf) with polynomial kernel based SVR (SVR_poly) models for both training data and testing data for stall torque ratio. The root mean squared error (RMSE) and correlation coefficient (R) served to evaluate the differences between the predicted and CFD simulation values for SVR_rbf and SVR_poly. A comparison between the SVR with RBF kernel results and the SVR with polynomial kernel results reveals that SVR with RBF kernel outperforms the SVR with polynomial kernel function in terms of estimation prediction for stall torque ratio.

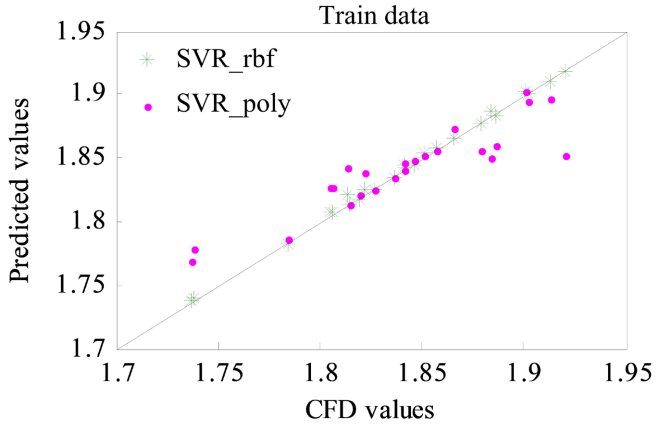

Figure 12. SVR prediction results for training data of stall torque ratio.

Figure 14 represents the results of the peak efficiency of CFD and predicted data in the preparation stage, while Figure 15 demonstrates the results for the testing stage. Both the SVR with RBF kernel and SVR with polynomial kernel perform well in estimating the peak efficiency. For stall peak efficiency prediction, the SVR with RBF kernel function has very small RMSE during training and this value is slightly larger in testing. The SVM with polynomial kernel have larger RMSE in training data and smaller RMSE in testing data than RBF. Table 4 compares

the SVR_rbf and SVR_poly models. It can be concluded that the SVR with RBF kernel is better than the SVR with polynomial kernel at estimating the performance characteristics of a torque converter.

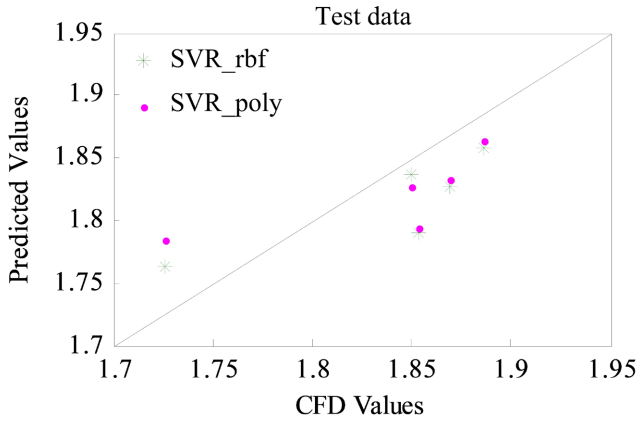

Figure 13. SVR prediction results for testing data of stall torque ratio.

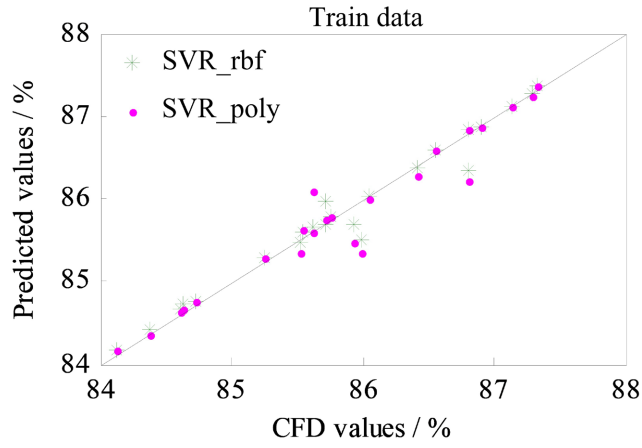

Figure 14. SVR prediction results for training data of peak efficiency.

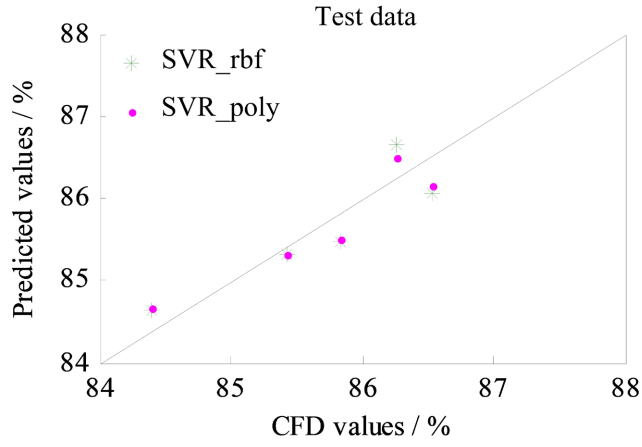

Figure 15. SVR prediction results for testing data of peak efficiency.

Table 4. SVR performance for prediction of stall torque ratio and peak efficiency.

Method	Stall torque ratio Tr_0				Peak efficiency η^* /%			
	Training		Testing		Training		Testing	
	RMSE	R	RMSE	R	RMSE	R	RMSE	R
SVR_rbf	0.000194	0.998621	0.062697	0.844790	0.002403	0.986141	0.024338	0.900186
SVR_poly	0.014299	0.910808	0.072086	0.764089	0.005023	0.971390	0.017835	0.933769

6. Conclusions

An attempt is made in this study to investigate the performance of support vector regression (SVR) technique for predicting torque converter performance including stall torque ratio and peak efficiency. The proposed method is verified by comparing the predicted values with CFD values. Two SVR models are investigated: radial basis function (SVR with RBF kernel) and polynomial function (SVR with polynomial kernel). According to RMSE and R parameters, it can be concluded that the SVR with RBF kernel is better than the SVR with polynomial kernel at estimating the performance of torque converter based on the turbine design parameters.

The prediction results demonstrate that SVR method can predict torque converter performance with higher estimation accuracy and generalization ability. Also according to results SVR may be a promising alternative to existing prediction models. It can be seen that the prediction model overcomes the main drawback of artificial neural networks without defining network structure and trapping in the local optimum.

Conflicts of Interest

The authors declare no conflicts of interest regarding the publication of this paper.

References

[1] Kim, G. and Jang, J. (2002) Effects of Stator Shapes on Hydraulic Performances of an Automotive Torque Converter with a Squashed Torus. *SAE* 2002 *World Congress & Exhibition*, Detroit, 4-7 March 2002, 8 p. https://doi.org/10.4271/2002-01-0886

[2] Gallimore, S.J. (1999) Axial Flow Compressor Design. *Proceedings of the Institution of Mechanical Engineers, Part C: Journal of Mechanical Engineering Science*, **213**, 437-449. https://doi.org/10.1243/0954406991522680

[3] Rutter, R., Sheth, K. and O'Bryan, R. (2013) Numerical Flow Simulation and Validation of an Electrical Submersible Pump. *Proceedings of the ASME* 2013 *Fluids Engineering Division Summer Meeting*, Incline Village, 7–11 July 2013, 7 p. https://doi.org/10.1115/fedsm2013-16078

[4] Zhao, B., Wang, Y., Chen, H., Qiu, J. and Hou, D. (2015) Hydraulic Optimization of a Double-Channel Pump's Impeller Based on Multi-Objective Genetic Algorithm. *Chinese Journal of Mechanical Engineering*, **28**, 634-640. https://doi.org/10.3901/cjme.2015.0116.016

[5] Shojaeefard, M.H., Tahani, M., Ehghaghi, M.B., Fallahian, M.A. and Beglari, M. (2012) Numerical Study of the Effects of Some Geometric Characteristics of a Cen-

trifugal Pump Impeller That Pumps a Viscous Fluid. *Computers & Fluids*, **60**, 61-70. https://doi.org/10.1016/j.compfluid.2012.02.028

[6] Bellary, S.A.I., Adhav, R., Siddique, M.H., Chon, B., Kenyery, F. and Samad, A. (2016) Application of Computational Fluid Dynamics and Surrogate-Coupled Evolutionary Computing to Enhance Centrifugal-Pump Performance. *Engineering Applications of Computational Fluid Mechanics*, **10**, 171-181. https://doi.org/10.1080/19942060.2015.1128359

[7] Hur, N., Moshfeghi, M. and Lee, W. (2018) Flow and Performance Analyses of a Partially-Charged Water Retarder. *Computers & Fluids*, **164**, 18-26. https://doi.org/10.1016/j.compfluid.2016.10.033

[8] Wu, G. (2008) System for Torque Converter Design and Analysis Based on Cad/CFD Integrated Platform. *Chinese Journal of Mechanical Engineering* (*English Edition*), **21**, 35-39. https://doi.org/10.3901/cjme.2008.04.035

[9] Dong, Y., Korivi, V., Attibele, P. and Yuan, Y. (2002) Torque Converter CFD Engineering Part I: Torque Ratio and K Factor Improvement through Stator Modifications. *SAE* 2002 *World Congress & Exhibition*, Detroit, 4-7 March 2002, 14. https://doi.org/10.4271/2002-01-0883

[10] Wu, G. and Wang, L. (2016) Application of Dual-Blade Stator to Low-Speed Ratio Performance Improvement of Torque Converters. *Chinese Journal of Mechanical Engineering*, **29**, 293-300. https://doi.org/10.3901/cjme.2015.1218.151

[11] Leng, Y., Xu, X. and Qi, G. (2013) Combining Active Learning and Semi-Supervised Learning to Construct SVM Classifier. *Knowledge-Based Systems*, **44**, 121-131. https://doi.org/10.1016/j.knosys.2013.01.032

[12] Qi, Z., Tian, Y., Shi, Y. and Yu, X. (2013) Cost-Sensitive Support Vector Machine for Semi-Supervised Learning. *Procedia Computer Science*, **18**, 1684-1689. https://doi.org/10.1016/j.procs.2013.05.336

[13] Chakraborty, S. (2011) Bayesian Semi-Supervised Learning with Support Vector Machine. *Statistical Methodology*, **8**, 68-82. https://doi.org/10.1016/j.stamet.2009.09.002

[14] Rajasekaran, S., Gayathri, S. and Lee, T.-L. (2008) Support Vector Regression Methodology for Storm Surge Predictions. *Ocean Engineering*, **35**, 1578-1587. https://doi.org/10.1016/j.oceaneng.2008.08.004

[15] Shamshirband, S., Petkovic, D., Javidnia, H. and Gani, A. (2015) Sensor Data Fusion by Support Vector Regression Methodology—A Comparative Study. *IEEE Sensors Journal*, **15**, 850-854. https://doi.org/10.1109/jsen.2014.2356501

[16] Taghavifar, H., Jafarmadar, S., Taghavifar, H. and Navid, A. (2016) Application of Doe Evaluation to Introduce the Optimum Injection Strategy-Chamber Geometry of Diesel Engine Using Surrogate Epsilon-SVR. *Applied Thermal Engineering*, **106**, 56-66. https://doi.org/10.1016/j.applthermaleng.2016.05.194

[17] Liu, S. (2009) Mathematical Model of Hydrodynamic Torque Converter and Analytic Description of Streamline. *Chinese Journal of Mechanical Engineering*, **22**, 70-77. https://doi.org/10.3901/cjme.2009.01.070

[18] Kęsy, A. and Kądziela, A. (2011) Construction Optimization of Hydrodynamic Torque Converter with Application of Genetic Algorithm. *Archives of Civil and Mechanical Engineering*, **11**, 905-920. https://doi.org/10.1016/s1644-9665(12)60086-7

[19] Wu, G.Q. and Wang, L.J. (2012) Performance Optimization of Torque Converters Based on Modified 1D Flow Model. *Journal of Donghua University*, **29**, 380-384.

[20] Wu, G. and Wang, L. (2015) Multi-Objective Optimization Employing Genetic Algorithm for the Torque Converter with Dual-Blade Stator. *SAE* 2015 *World Congress*

& Exhibition, Detroit, 21-23 April 2015, 10. https://doi.org/10.4271/2015-01-1119

[21] Ch, S., Anand, N., Panigrahi, B.K. and Mathur, S. (2013) Streamflow Forecasting by SVM with Quantum Behaved Particle Swarm Optimization. *Neurocomputing*, **101**, 18-23. https://doi.org/10.1016/j.neucom.2012.07.017

[22] Wang, W., Chau, K., Cheng, C. and Qiu, L. (2009) A Comparison of Performance of Several Artificial Intelligence Methods for Forecasting Monthly Discharge Time Series. *Journal of Hydrology*, **374**, 294-306. https://doi.org/10.1016/j.jhydrol.2009.06.019

[23] Asefa, T., Kemblowski, M., McKee, M. and Khalil, A. (2006) Multi-Time Scale Stream Flow Predictions: The Support Vector Machines Approach. *Journal of Hydrology*, **318**, 7-16. https://doi.org/10.1016/j.jhydrol.2005.06.001

[24] Spence, R. and Amaral-Teixeira, J. (2009) A CFD Parametric Study of Geometrical Variations on the Pressure Pulsations and Performance Characteristics of a Centrifugal Pump. *Computers & Fluids*, **38**, 1243-1257. https://doi.org/10.1016/j.compfluid.2008.11.013

[25] Steinberg, D.M. and Lin, D.K.J. (2006) A Construction Method for Orthogonal Latin Hypercube Designs. *Biometrika*, **93**, 279-288. https://doi.org/10.1093/biomet/93.2.279

[26] Schölkopf, B. and Smola, A.J. (2001) Learning with Kernels: Support Vector Machines, Regularization, Optimization, and beyond. The MIT Press. https://doi.org/10.7551/mitpress/4175.001.0001

[27] Shamshirband, S., Petković, D., Amini, A., Anuar, N.B., Nikolić, V., Ćojbašić, Ž., *et al.* (2014) Support Vector Regression Methodology for Wind Turbine Reaction Torque Prediction with Power-Split Hydrostatic Continuous Variable Transmission. *Energy*, **67**, 623-630. https://doi.org/10.1016/j.energy.2014.01.111

[28] Vapnik, V. (2013) The Nature of Statistical Learning Theory. Springer Science & Business Media.

[29] Brereton, R.G. and Lloyd, G.R. (2010) Support Vector Machines for Classification and Regression. *The Analyst*, **135**, 230-267. https://doi.org/10.1039/b918972f

[30] Petković, D., Shamshirband, S., Saboohi, H., Ang, T.F., Anuar, N.B. and Pavlović, N.D. (2014) RETRACTED ARTICLE: Support Vector Regression Methodology for Prediction of Input Displacement of Adaptive Compliant Robotic Gripper. *Applied Intelligence*, **41**, 887-896. https://doi.org/10.1007/s10489-014-0574-5

[31] Hsu, C.W., Chang, C.C. and Lin, C.J. (2003) A Practical Guide to Support Vector Classification.

[32] Duan, K., Keerthi, S.S. and Poo, A.N. (2003) Evaluation of Simple Performance Measures for Tuning SVM Hyperparameters. *Neurocomputing*, **51**, 41-59. https://doi.org/10.1016/s0925-2312(02)00601-x

[33] Keerthi, S.S. (2002) Efficient Tuning of SVM Hyperparameters Using Radius/Margin Bound and Iterative Algorithms. *IEEE Transactions on Neural Networks*, **13**, 1225-1229. https://doi.org/10.1109/tnn.2002.1031955

[34] Lin, P.T. (2001) Support Vector Regression: Systematic Design and Performance Analysis.

[35] Chen, N., Lu, W., Yang, J. and Li, G. (2004) Support Vector Machine in Chemistry. World Scientific. https://doi.org/10.1142/5589